ISSN 1027-5495. Functional Materials, 28, No.2 (2021), p. 245-251.
doi:https://doi.org/10.15407/fm28.02.245 © 2021 — STC "Institute for Single Crystals"

Electrical properties of photosensitive n–SnS_2/p–InSe heterostructures fabricated by spray pyrolysis

***I.G.Orletskii*[1], *I.G.Tkachuk*[2], *Z.D.Kovalyuk*[2], *P.D.Maryanchuk*[1], *V.I.Ivanov*[2]**

[1]Y.Fedkovych Chernivtsi National University,
2 Kotsyubynsky Str., 58012 Chernivtsi, Ukraine
[2]I.Frantsevich Institute for Problems of Materials Science,
Chernivtsi Branch, National Academy of Sciences of Ukraine,
5 I.Vilde Str., 58001 Chernivtsi, Ukraine

Received September 12, 2020

The conditions for the fabrication of photosensitive anisotypic n–SnS_2/p–InSe heterojunctions by the method of spray pyrolysis of thin films on crystalline p–InSe substrates are studied. On the basis of analysis of temperature dependences of the forward and reverse I–V characteristics, the energy parameters of the heterojunction and the mechanisms of current generation in the heterostructure are calculated. A model for determining the height of the energy barrier in the structures with high resistance of the base region is proposed. The profile of the energy diagram of the heterostructure is drawn, which agrees well with the experimentally observed electro-physical phenomena. The processes of photocurrent generation in the heterostructure are analyzed.
Keywords: heterostructures, photosensitivity, photocurrent, spray pyrolysis, thin films, indium selenide, tin (IV) sulfide.

Електричні властивості фоточутливих гетероструктур n–SnS_2/p–InSe, виготовлених методом спрей-піролізу. *І.Г.Орлецький, І.Г.Ткачук, З.Д.Ковалюк, П.Д.Мар'янчук, В.І.Іванов*

Досліджено умови виготовлення фоточутливих анізотипних гетеропереходів n–SnS_2/p–InSe методом спрей-піролізу тонких плівок SnS_2 на кристалічні підкладки p–InSe. За аналізом температурних залежностей прямих і зворотних I–V-характеристик визначено енергетичні параметри гетеропереходу та механізми формування струмів у гетероструктурі. Запропоновано модель визначення висоти енергетичного бар'єру у структурах з високим опором базової області. Встановлено профіль енергетичної діаграми гетероструктури, яка добре узгоджується із спостережуваними експериментально електрофізичними явищами. Проаналізовано процеси утворення фотоструму у гетероструктурі.

Исследованы условия изготовления фоточувствительных анизотипних гетеропереходов n–SnS_2/p–InSe методом спрей-пиролиза тонких пленок SnS_2 на кристаллические подложки p–InSe. Из анализа температурных зависимостей прямых и обратных I–V-характеристик определены энергетические параметры гетероперехода и механизмы формирования токов в гетероструктуре. Предложена модель определения высоты энергетического барьера в структурах с высоким сопротивлением базовой области. Приведено профиль энергетической диаграммы гетероструктуры, которая хорошо согласуется с экспериментально наблюдаемыми электрофизическими явлениями. Проанализировано процессы образования фототока в гетероструктуре.

1. Introduction

Thin films of tin sulfides (SnS, SnS_2, Sn_2S_3) are characterized by different phase composition, which determines their basic physical properties. The tin (IV) sulfide (SnS_2) films with a band gap width of $E_g \approx 2.45$ eV [1] are suitable for the fabrication of the front layer of photodetectors based on heterojunctions. The SnS_2 film contains chemical elements Sn and S, which are widespread, low cost and low toxicity. A number of photosensitive structures based on SnS_2 films have already been fabricated and investigated: n–SnS_2/p–SnS [2, 3], SnO_2/SnS_2 [4] and n–SnS_2/p–Si [5].

For the fabrication of the tin disulfide films, preference is given to inexpensive non-vacuum methods of spray pyrolysis of chemical solutions of Sn and S salts [5, 6], spin-coating deposition from organotin sulfides [7], and a facile chemical bath deposition method [8]. These methods provide the necessary modes of sulfide films deposition [9, 10] with desired physical properties.

The indium monoselenide with a band gap width of 1.2 eV is a suitable material for photoelectric energy conversion in terrestrial conditions. The layered structure of InSe crystals with a weak van der Waals bond simplifies the fabrication of substrates for heterostructures and eliminates the need to cut ingots into plates and their mechanical and chemical processing. Photosensitive and diode structures of various types have already been created on the basis of indium selenide: Schottky and p–n diodes [11], p–n junctions [12, 13], and heterojunctions [14–17].

The n–SnS_2/p–InSe heterojunctions fabricated by the method of optical contact of semiconductors with the appearance of an inversion layer in p–InSe have good photoelectric properties. But they need a SnS_2 bulk crystal. The properties of the n–SnS_2/p–InSe heterojunction largely depend on the manufacturing method. The use of spray pyrolysis of SnS_2 films eliminates the need to grow bulk SnS_2 material. This method is accompanied by thermal processes of decomposition of chloride salts on the p–InSe surface with a possible change in the properties of the substrate surface, which is reflected in the properties of the formed SnS_2/p–InSe heterojunction.

This paper presents the results of the study of electrical properties and spectral photosensitivity of the n–SnS_2/p–InSe heterojunction fabricated by spray pyrolysis of tin (IV) sulfide thin films on p–InSe substrates. Among other tin sulfides, SnS_2 is the best candidate for the formation of a heterojunction with InSe due to its optimal band gap. SnS_2 is transparent at the maximum spectral sensitivity of InSe (1.2÷2.5 eV), which, on the one hand, allows the most efficient use of InSe, and, on the other hand, increases the photosensitivity of the heterojunction in the region > 2.4 eV due to absorption in SnS_2.

2. Experimental

To fabricate the n–SnS_2/p–InSe heterostructures we used the p–InSe substrate grown by the Bridgman method. The p-type conductivity of InSe was provided by cadmium doping (0.1 wt. %). According to the study of the Hall effect in InSe, the concentration of charge carriers is $p \approx 10^{14}$ cm^{-3} and hole mobility across the c axis is $\mu_{pH} \approx 50$ cm^2/(V·s) at 295 K.

The n–SnS_2/p–InSe heterostructures were fabricated by deposition of SnS_2 films with a thickness of 0.3÷0.4 μm on the surface of p–InSe substrates heated to $T_S = 623$ K by spray pyrolysis of aqueous solutions of salts of tin (IV) chloride pentahydrate ($SnCl_4 \cdot 5H_2O$) and thiourea ($(NH_2)_2CS$) at atmospheric pressure of 0.1 MPa. During pyrolysis, a binary n–SnS_2 compound with electrical conductivity of $\sigma \approx 3 \cdot 10^{-1}$ $\Omega^{-1} \cdot$cm^{-1} and a band gap width of $E_g = 2.4$ eV is formed [3]. There are no features in the spectral dependence that would indicate SnS or Sn_2S_3, but there is an increase in photosensitivity at $h\nu \geq 2.4$ eV (the edge of self-absorption in SnS_2). The grown n–SnS_2 films are polycrystalline. Taking into account a low value of electron mobility ($\mu = 2.43 \cdot 10^{-3}$ cm$^2 \cdot$V^{-1}s^{-1}) in polycrystalline films [6], the concentration of free charge carriers in SnS_2 films is $n \approx 2.7 \cdot 10^{17}$ cm^{-3}.

The contacts to the p–InSe and n–SnS_2 film were made using a silver-based conductive paste. The I–V characteristics of the n–SnS_2/p–InSe heterostructures were measured with a SOLARTRON SI 1286, SI 1255 complex in the temperature range from 243 K to 333 K. The photosensitivity spectra of the heterojunctions were studied at room temperature using an MDR 3 monochromator with a resolution of 2.6 nm/mm. The spectra were normalized relative to the photon flux.

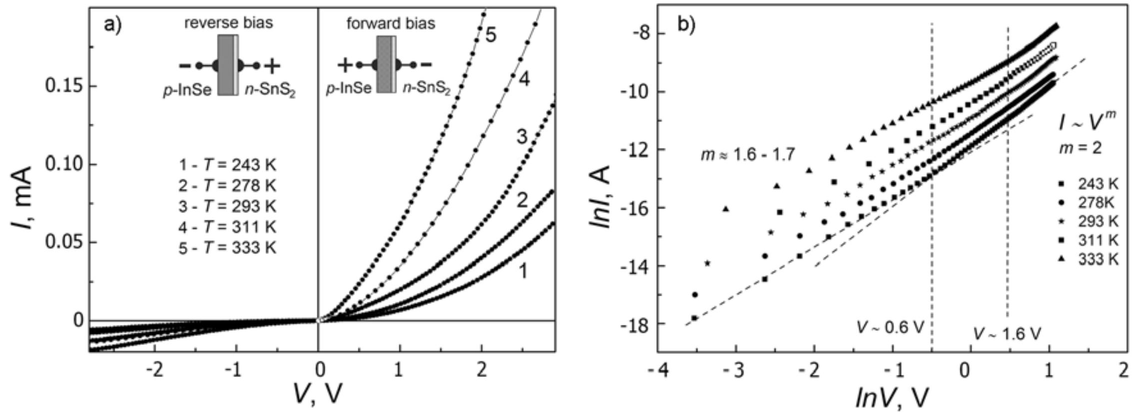

Fig. 1. I–V characteristics of the n–SnS_2/p–InSe heterostructure.

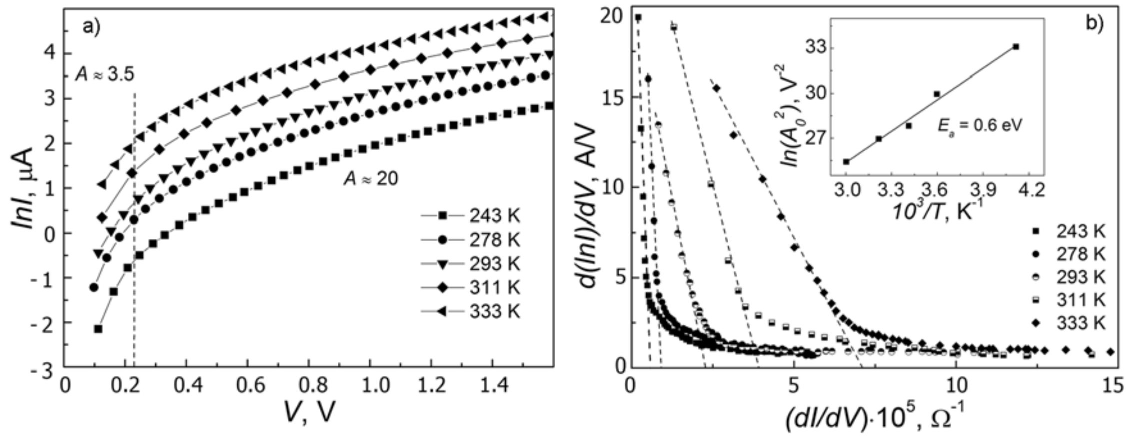

Fig. 2. I–V characteristics of the n–SnS_2/p–InSe heterostructure at forward bias. The insert shows the calculation of activation energy (E_a) in SnS_2 film.

3. Results and discussion

The study of the I–V characteristics in the voltage range from −3 V to 3 V at temperatures from 243 K to 333 K indicated the ability of the n–SnS_2/p–InSe heterostructure to rectify the current (Fig. 1). A forward bias of the heterojunction corresponded to applying positive voltage to the p–InSe base region, and a reverse bias corresponded to applying positive voltage to the n–SnS_2 film.

The current in the p–InSe base region of the n–SnS_2/p–InSe heterostructure flows in a direction perpendicular to the plane of the crystal layers. This causes the emergence of a significant series resistance (R_s) in the structure. Due to a decrease in the resistance of the heterojunction at forward bias, starting from a certain value, all external voltage is applied to the high-impedance p–InSe base region. Then the space charge limited (SCL) current appears [19]:

$$I_{SCL} = \frac{9\varepsilon_S\varepsilon_0 V^2}{8L^3}, \quad (1)$$

where L is the length of the space charge region, ε_S is the dielectric constant of the semiconductor.

In this case, according to Eq. 1, the I–V characteristic at forward bias is linear in the coordinates of $\ln I = f(\ln V)$ with an angle of inclination $\mathrm{tg}\beta = m = 2$. In the n–SnS_2/p–InSe heterostructure, the SCL regime appears at voltages greater than 0.6 V (Fig. 1b).

The resistance of the base region decreases with an increase in temperature and a larger forward bias voltage is required for appearance of the SCL regime. As can be seen from Fig. 1b, at T = 333 K, the SCL regime is observed at voltages greater than 1.6 V. At lower voltages, when m decreases to 1.6÷1.7, the current in the structure is determined by the energy barrier at the n–SnS_2/p–InSe interface.

In order to elucidate the current flow mechanism in the n–SnS_2/p–InSe hetero-

junction, the I–V characteristics were analyzed in the voltage range from $3kT/q$ to 1.6 V (Fig. 2). In the temperature range from 243 to 333 K, the dependences $\ln I = f(V)$ have a temperature independent slope $(d(\ln I)/dV)$. The I–V characteristics are described by the following expression:

$$I(V) = I_S \exp\left(\frac{qV}{AkT}\right), \quad (2)$$

where A is the coefficient of imperfection, that varies from 3.5 to 20. The high values of A in the p–Ge/n–Si heterojunctions (A = 24.9÷29.4) are the result of tunnel or tunnel recombination mechanisms of current flow through the barrier of height φ_B, that are described by the expression [20]:

$$I(V) = BN_i \exp[-A_0(\varphi_B - V)], \quad (3)$$

where B is the some constant, N_t is the concentration of traps in the band gap, A_0 is the value that depends on the concentration of impurities N in the semiconductor from which the tunneling proceeds:

$$A_0 = \frac{4}{3\hbar}\left(\frac{m_0\varepsilon_S}{N}\right)^{1/2}. \quad (4)$$

Taking into account the voltage drop across the series resistance of the base region, the voltage at the heterojunction is equal to $V - IR_S$ and Eq. 3 takes the form:

$$I(V) = BN_i(\exp)[-A_0(\varphi_B - V + IR_S)]. \quad (5)$$

From Eq. 1 we find the expression for the analysis of current generation mechanism at forward bias:

$$\frac{d(\ln I)}{dV} = -A_0\left(\frac{d(\varphi_B - V)}{dV} + \frac{dI \cdot R_S}{dV}\right). \quad (6)$$

In the case when the voltage drop across the heterojunction is greater than the voltage drop across the series resistance ($\varphi_B - V > IR_S$), the external voltage applied to the heterojunction and Eq. 6 could be written as:

$$\frac{d(\ln I)}{dV} = -A_0\left(\frac{d(\varphi_B - V)}{dV}\right). \quad (7)$$

In the case of decreasing the resistance of the heterojunction ($(\varphi_B - V) \to 0$), the Eq. 6 is linear with an inclination to the abscissa axis of A_0R_S.

The $d(ln(I))/dV = f(dI/dV)$ dependence for the n–SnS_2/p–InSe heterostructure at forward bias has two linear portions (Fig. 2b). At low rates of current change with voltage (dI/dV), the value of $d(ln(I))/dV$ rapidly decreases due to a decrease in the resistance of the heterojunction. When the resistance of the heterojunction becomes less than the series resistance, the dynamics of change in the value of $d(ln(I))/dV$ slows down and is determined by the series resistance.

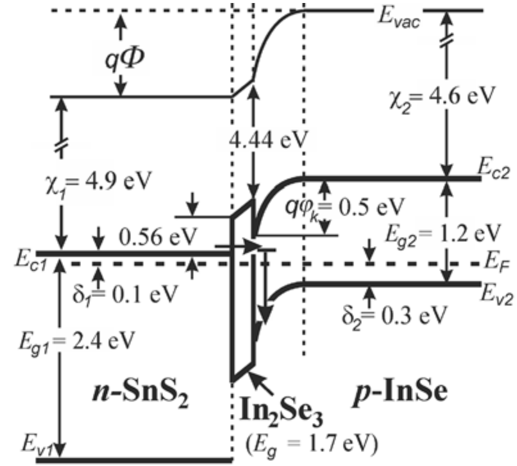

Fig. 3. Energy diagram of the n–SnS_2/p–InSe heterojunction (T = 300 K) with an energy barrier of $q\varphi_B$ = 0.56 eV (barrier height is independent from temperature).

According to Eq. 7, the value of dI/dV at which $(\varphi_B - V) = 0$ could be obtained by extrapolating of the linear portion of $d(ln(I))/dV$ to the x-axis. The values of the voltage at the heterojunction do not depend on temperature and are equal to φ_B: $V = \varphi_B = 0.5$ V. This indicates that at low forward bias voltage (up to 0.5 V) the current in the n–SnS_2/p–InSe heterostructure is formed by tunneling through an energy barrier with a height of $q\varphi_B \approx 0.5$ eV, which does not depend on temperature.

Fig. 3 shows the energy diagram used to analyze the electrical properties of the n–SnS_2/p–InSe heterojunction. It assumes the existence of an energy barrier with a temperature-independent height at the interface between semiconductors. The following data were used to construct the energy diagram: electron affinity $\chi(SnS_2)$ = 4.9 eV [21], χ(InSe) = 4.55÷4.6 eV [22–25], $E_g(SnS_2)$ = 2.4 eV [26] and E_g(InSe) = 1.2 eV [27]. The value of $E_g(SnS_2)$ corresponds to the experimental value for the films obtained by spray pyrolysis at a temperature of T_S = 623 K. There is a change in the phase composition of the substrate surface [14, 28] due to heating in some cases during fabrication of

heterostructures by spray pyrolysis. The influence of a tunnel-thin In_2Se_3 layer on the properties of a p–InSe-based heterojunction is analyzed in [14]. The energy characteristics of In_2Se_3 ($E_g \approx 1.7$ eV [29, 30] and $\chi = 4.44$ eV [31]) agree well with the energy barrier height of $q\varphi_B \approx 0.5$ eV, which is experimentally observed in the n–SnS_2/p–InSe heterojunction.

The location of the Fermi level relative to bottom of the n–SnS_2 conduction band (δ_1 = 0.1 eV) and the top of the p–InSe valence band (δ_2 = 0.3 eV) was calculated from the expressions for the equilibrium concentration of charge carriers of nondegenerate semiconductors [32]. The contact potential difference (φ_k) appears at the n–SnS_2/p–InSe interface due to the difference in the electron work functions: $\varphi_k = (\chi_2 + E_{g2} - \delta_2) - (\chi_1 + E_{g1}) = 0.5$ eV. According to the calculations [33], φ_k is concentrated in the contact region of p–InSe.

The tunneling mechanism of electrons from the bottom of the n–SnS_2 conduction band through a barrier height of $q\varphi_B$ = 0.56 eV (Fig. 3) to the levels in the band gap of p–InSe, which are located at distance of 0.3÷0.4 eV from the conduction band bottom, is well consistent with the nature of these levels. According to [34], they are associated with anion vacancies in InSe, which occur due to heating of the substrate during spray pyrolysis. Other possible current mechanisms are in poor agreement with the experiment.

In the absence of a In_2Se_3 layer, the capture of electrons by states at the interface and tunneling into the valence band are presupposes the dependence of a barrier height ($q\varphi_k$) from temperature, which is not observed. The temperature-independent height of the barrier at the n–SnS_2/p–InSe interface could exist due to the rupture of the conduction band, but it is much smaller than observed experimentally ($\chi_1 - \chi_2 = 0.3$ eV).

The tunnel transparency W of a barrier with a height of $q\varphi_B = 0.56$ eV is calculated according to the following expression [35]:

$$W = \exp\left(-\frac{2d}{\hbar}\sqrt{2m^*\varphi_B}\right), \quad (8)$$

where W varies from 1 at a thickness of the In_2Se_3 film $d = 0.3$ nm to 0.05 at d = 0.6 nm. That is, the experimentally observed tunneling ability will occur at the thickness of the In_2Se_3 film d = 0.3÷0.6 nm.

The temperature dependence of the angle of inclination of the linear portions (Fig. 2b), which were used to determine an energy barrier height ($q\varphi_B \approx 0.5$ eV) at the n–SnS_2/p–InSe heterojunction is associated with an increase in electron concentration in n–SnS_2. The dependence of $\ln(A^2) = f(10^3/T)$ allows calculation of the activation energy of the electrical conductivity (E_a) in the film (see insert to Fig. 2b). The obtained value of E_a = 0.6 eV agrees well with the known data for both bulk [36] and thin-film [37] SnS_2 semiconductor.

The I–V characteristics of the n–SnS_2/p–InSe heterojunction at reverse bias are investigated in the temperatures range from 243 K to 333 K and the reverse voltages range from −3 V to 0 V. They can be described by the following expression for tunnel current [20]:

$$I = a_0\exp(-b_0(\varphi_B - V)^{-1/2}), \quad (9)$$

where a_0 is a parameter determined by the probability of filling the energy levels from which the tunneling occurs, and b_0 is determined by the rate of change of current versus voltage.

According to Eq. 9, the I–V characteristic is linear in the coordinates $\ln I = f(\varphi_B - V)^{-1/2}$ (Fig. 4). At voltages from −3 V to 0 V, the reverse current in the n–SnS_2/p–InSe heterostructure is generated by tunneling electrons from the conduction band bottom and energy states of the p–InSe band gap ($E_{C2} - E_F = 0.3 - 0.4$ eV) to the n–SnS_2 conduction band through the energy barrier formed by In_2Se_3.

Fig. 5 shows the spectral dependence of the quantum efficiency of the n–SnS_2/p–InSe heterostructure in the photon energy ($h\nu$) range from 1.2 eV to 3.2 eV. The light falls on the SnS_2 film side. The maximum of the quantum efficiency is at 1.7 eV. The long-wavelength edge of photosensitivity at $h\nu$ = 1.2 eV is due to the edge of fundamental absorption in p–InSe. The tunnel-thin barrier of In_2Se_3 separates the electrons photogenerated in p–InSe (1 in the insert to Fig. 5). As a result of the fact that n–SnS_2 thin films are polycrystalline, the intrinsic absorption edge is blurred due to partial absorption at the grain boundaries compared to single-crystalline materials [26]. At energies $h\nu < E_g = 2.4$ eV, part of the radiation is absorbed at the grain boundaries. In this case, light does not penetrate into the base p–InSe region due to absorption in n–SnS_2

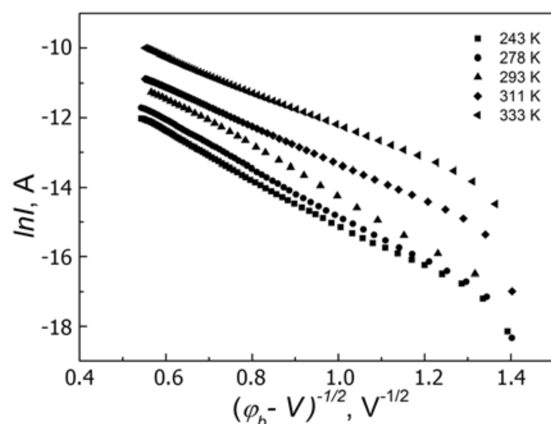

Fig. 4. *I–V* characteristics of the n–SnS_2/p–InSe heterostructure at reverse bias.

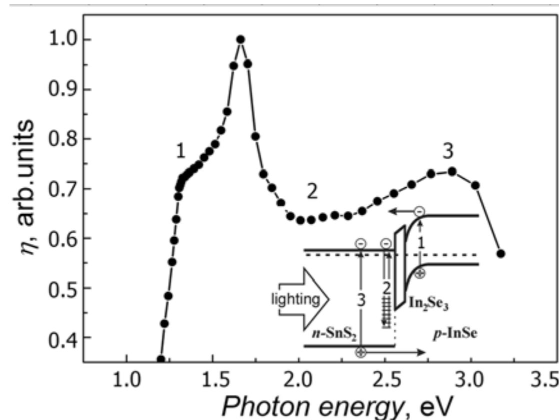

Fig. 5. Spectral dependence of relative quantum efficiency of the n–SnS_2/p–InSe heterostructure.

without the formation of minority charge carriers (2 in the insert to Fig. 5). This causes a decrease in photocurrent and photosensitivity (area 2 in the Fig. 5). At energies $h\nu > 2.4$ eV, free minority carriers are generated in the n–SnS_2 film. They diffuse to the heterojunction and generate current. The photosensitivity increases (area 3 in the Fig. 5). The width of the half-height of the spectrum of the relative quantum efficiency is $\delta_{1/2} \approx 1.8$.

4. Conclusions

The photosensitive n–SnS_2/p–InSe structures were fabricated by the method of spray pyrolysis of SnS_2 films on the p–InSe substrates. The diode properties of the structures are determined by the difference between the energy parameters of n–SnS_2 and p–InSe and the energy barrier of a In_2Se_3 tunnel-thin layer with a temperature-independent height of $q\varphi_B \approx 0.5$ eV. At forward bias voltage $V < 0.6$ V ($T \approx 290$ K), the main current mechanism is the tunneling of electrons from the n–SnS_2 conduction band bottom through the barrier to states in the p–InSe band gap with the following recombination. The tunnel current increases with temperature due to an increase in the electron concentration in the n–SnS_2 conduction band. At forward bias voltage $V >$ 0.6 V ($T \approx 290$ K), the decrease in external voltage focuses on the high-impedance p–InSe base region and the space charge limiting mechanism is implemented. With increasing temperature, the voltage at which the space charge limiting mechanism observed increases to $V = 1.6$ V ($T \approx 330$ K). The reverse current in the n–SnS_2/p–InSe heterostructure is generated by the tunneling of electrons from the conduction band bottom and energy states of the p–InSe band gap to the n–SnS_2 conduction band through the energy barrier formed by In_2Se_3.

The n–SnS_2/p–InSe heterostructures are photosensitive in the range from 1.2 eV to 3.2 eV and could be used for fabrication of photo-detectors if the non-photoactive absorption in the n–SnS_2 film is reduced.

References

1. Y.Huang, E.Sutter, J.T.Sadowski et al., *ACS Nano*, **8**, 10743 (2014).
2. A.Sanchez-Juarez, A.Tiburcio-Silver, A.Ortiz, *Thin Sol.Films*, **480**, 452 (2005).
3. A.Degrauw, R.Armstrong, A.A.Rahman et al., *Mater.Res.Express*, **4**, 094002 (2017).
4. H.Chen, M.Gu, X.Pu et al., *Mater.Res.Express*, **3**, 065002 (2016).
5. G.M.Kumar, F.Xiao, P.Ilanchezhiyan et al., *RSC Adv.*, **6**, 99631 (2016).
6. M.R.Fadavieslam, *J.of Mater.Sci.:Mater.in Electron.*, **28**, 2392 (2017).
7. T.Ricica, L.Strizik, L.Dostal et al., *Appl.Org. Chem.*, **29**, 176 (2015).
8. S.Gedi, V.R.Minnam Reddy, B.Pejjai et al., *Ceramics International.*, **43**, 3713 (2017).
9. I.G.Orletskii, P.D.Mar'yanchuk, E.V.Maistruk et al., *Fiz.Tverd.Tela*, **58**, 39 (2016).
10. I.G.Orletskii, M.N.Solovan, F.Pinna et al., *Fiz.Tverd.Tela*, **59**, 783 (2017).
11. A.Segura, J.P.Guesdon, J.M.Besson, *A.Chevy. Rev.Phys.Appl.*, **14**, 253 (1979).
12. V.A.Khandozhko, Z.R.Kudrynskyi, Z.D.Kovalyuk, *Fiz.Tekh.Poluprovodn.*, **48**, 564 (2014).
13. A.Segura, J.P.Guesdon, J.M.Besson, A.Chevy, *J.Appl.Phys.*, **54**, 876 (1983).
14. I.G.Orletsky, M.I.Ilashchuk, V.V.Brus et al., *Fiz.Tekh.Poluprovodn.*, **50**, 339 (2016).

15. Z.R.Kudrynskyi, Z.D.Kovalyuk, V.M.Katerynchuk et al., *Acta Phys.Pol.A*, **124**, 720 (2013).
16. V.N.Katerynchuk, Z.R.Kudrynskyi, V.V.Khomyak et al., *Fiz.Tekh.Poluprovodn.*, **47**, 935 (2013).
17. I.G.Tkachuk, I.G.Orletsky, Z.D.Kovalyuk, P.D.Marianchuk, *Functional Materials*, **25**, 463 (2018).
18. V.N.Katerinchuk, M.Z.Kovalyuk, *J.Adv. Mater.*, **4**, 40 (1997).
19. M.A.Lampert, P.Mark, Current Injection in Solids, Academic Press, New York (1970).
20. A.G.Milnes, D.L.Feucht, Heterojunctions and Metal-semiconductor Junctions, Academic Press, New York (1972).
21. L.A.Burton, D.Colombara, R.D.Abellon et al., *Chem.Mater.*, **25**, 4908 (2013).
22. G.W.Mudd, S.A.Svatek, L.Hague et al., *Adv. Mater.*, **27**, 3760 (2015).
23. F.Yan, L.Zhao, A.Patane et al., *Nanotechnology*, **28**, 02534 (2017).
24. M.K.L.Man, A.Margiolakis, S.Deckoff-Jones et al., *Nat.Nanotech.*, **12**, 36 (2016).
25. S.E.Al Garni, O.A.Omareye, A.F.Qasrawi, *Optik*, **144**, 340 (2017).
26. I.G.Orletskii, P.D.Maryanchuk, E.V.Maistruk et al., *Neorg.Mater.*, **52**, 914 (2016).
27. Z.D.Kovalyuk, O.N.Sydor, V.N.Katerinchuk, V.V.Netyaga, *Fiz.Tekh.Poluprovodn.*, **41**, 1074 (2007).
28. I.G.Orletskyi, M.I.Ilashchuk, E.V.Maistruk et al., *Ukr.J.Phys.*, 64, 161 (2019).
29. R.Vaidyanathan, J.L.Stickney, S.M.Cox et al., *J.Electroanal.Chem.*, **559**, 55 (2003).
30. S.B.Bansode, R.S.Kapadnis, A.S.Ansari et al., *J.Mater.Sci.:Mater.Electron.*, **27**, 12351 (2016).
31. Z.Zheng, J.Yao, G.Yang, *ACS Appl.Mater.Interfaces*, **9**, 7288 (2017).
32. S.M.Sze, K.N.Kwok, Physics of Semiconductor Devices, Wiley, Durham, North Carolina (2006).
33. B.L.Sharma, R.K.Purohit, Semiconductor Heterojunctions, Pergamon Press, New York (1974).
34. M.A.Mehrabova, R.S.Madatov, *Fiz.Tekh. Poluprovodn.*, **45**, 1031 (2011).
35. I.G.Orletskyi, M.M.Solovan, V.V.Brus et al., *J.Phys.Chem.Solids*, **100**, 154 (2017).
36. S.G.Patil, R.H.Tredgold, *J.Phys.D: Appl. Phys.*, **4**, 718 (1971).
37. A.Voznyi, V.Kosyak, A.Opanasyuk et al., *Mater.Chem.Phys.*, **173**, 52 (2016).